OFFICE OF NAVAL RESEARCH

Grant No. _____

R&T Code N00014-92-C-0173

Technical Report #05

IN SITU FOURIER TRANSFORM INFRARED SPECTROSCOPIC STUDY OF BISULFATE AND SULFATE ADSORPTION ON GOLD, WITH AND WITHOUT THE UNDERPOTENTIAL DEPOSITION OF COPPER

by

Diane B. Parry
Mahesh G. Samant
H. Seki
Michael R. Philpott
Kevin Ashley*

Prepared for publication

in the

Journal of Physical Chemistry

IBM Research Division, Almaden Research Center,
650 Harry Road, San Jose, CA 95120-6099

1993

*Department of Chemistry, San Jose State University, San Jose, California 95192

SECURITY CLASSIFICATION OF THIS PAGE *(When Data Entered)*

REPORT DOCUMENTATION PAGE		READ INSTRUCTIONS BEFORE COMPLETING FORM
1. REPORT NUMBER 05	2. GOVT ACCESSION NO	3. RECIPIENT'S CATALOG NUMBER
Technical Report 16 4. TITLE *(and Subtitle)* In Situ Fourier Transform Infrared Spectroscopic Study of Bisulfate and Sulfate Adsorption on Gold, With and Without the Underpotential Deposition of Copper		5. TYPE OF REPORT & PERIOD COVERED Technical Report 6. PERFORMING ORG. REPORT NUMBER
7. AUTHOR(s) Diane B. Parry Mahesh G. Samant H. Seki M. R. Philpott, Kevin Ashley		8. CONTRACT OR GRANT NUMBER(s) N00014-92-C-0173
9. PERFORMING ORGANIZATION NAME AND ADDRESS IBM Research Division, Almaden Research Center 650 Harry Road San Jose, CA 95120-6099		10. PROGRAM ELEMENT, PROJECT, TASK AREA & WORK UNIT NUMBERS
11. CONTROLLING OFFICE NAME AND ADDRESS Office of Naval Research 800 North Quincy Street Arlington, VA 22217		12. REPORT DATE 4/14/93 13. NUMBER OF PAGES 46
14. MONITORING AGENCY NAME & ADDRESS *(If different from Controlling Office)* Dr. Ronald A. De Marco Office of Naval Research, Chemistry Division 800 N. Quincy Street Arlington, VA 22217 U.S.A.		15. SECURITY CLASS *(of this report)* Unclassified 15a. DECLASSIFICATION/DOWNGRADING SCHEDULE

16. DISTRIBUTION STATEMENT *(of this Report)*
Approved for public release; unlimited distribution.

17. DISTRIBUTION STATEMENT *(of the abstract entered in Block 20, if different from Report)*
Approved for public release; unlimited distribution.

18. SUPPLEMENTARY NOTES
Prepared for publication in Journal of Physical Chemistry

19. KEY WORDS *(Continue on reverse side if necessary and identify by block number)*

20. ABSTRACT *(Continue on reverse side if necessary and identify by block number)*
SEE NEXT PAGE

SECURITY CLASSIFICATION OF THIS PAGE *(When Data Entered)*

In situ surface infrared (IR) spectroelectrochemistry is used to investigate the adsorption of sulfate (SO_4^{2-}) and bisulfate (HSO_4^-) ions on polycrystalline gold surfaces in sodium sulfate and sulfuric acid, and also during copper underpotential deposition in sulfuric acid medium. In sodium sulfate solution, IR peaks due to surface sulfate and bisulfate are observed at potentials within the double-layer region on gold, and the ratio of IR peak intensities for sulfate to bisulfate increases as the applied potential is made more negative. In sulfuric acid, surface IR spectra indicate that adsorbed sulfate is favored at more positive potentials, while adsorbed bisulfate is prevalent at more negative voltages; also, a potential-dependent reorientation of water is observed in the spectra. IR spectroelectrochemical data from a sulfuric acid system containing copper sulfate indicate that adsorbed sulfate is present on gold at more positive potentials, and its coverage increases when underpotentially deposited (UPD) copper is present on the gold substrate surface. When the applied potential is sufficiently negative to effect full discharge of UPD copper, IR spectroelectrochemistry shows a loss of adsorbed sulfate and an increase in surface bisulfate species, with a concomitant reorientation of adsorbed water molecules. The results are explained in terms of surface electrostatic considerations during UPD of copper, and also in terms of potential-dependent pH changes at the interface. To our knowledge, this is the first reported infrared spectroelectrochemical study of interfacial changes occurring during metal underpotential deposition processes.

IN SITU FOURIER TRANSFORM INFRARED SPECTROSCOPIC STUDY OF BISULFATE AND SULFATE ADSORPTION ON GOLD, WITH AND WITHOUT THE UNDERPOTENTIAL DEPOSITION OF COPPER

Diane B. Parry,[#] Mahesh G. Samant, H. Seki, and M. R. Philpott[*]

IBM Research Division
Almaden Research Center
San Jose, California 95120

Kevin Ashley[@]

Department of Chemistry
San Jose State University
San Jose, California 95192

[#]Current address: Procter & Gamble Company, Ivorydale Technical Center, St. Bernard, OH 45217

[@]Current address: National Institute for Occupational Safety & Health, Division of Physical Sciences & Engineering, Cincinnati, OH 45226

[*]Author for correspondence

ABSTRACT

In situ surface infrared (IR) spectroelectrochemistry is used to investigate the adsorption of sulfate (SO_4^{2-}) and bisulfate (HSO_4^-) ions on polycrystalline gold surfaces in sodium sulfate and sulfuric acid, and also during copper underpotential deposition in sulfuric acid medium. In sodium sulfate solution, IR peaks due to surface sulfate and bisulfate are observed at potentials within the double-layer region on gold, and the ratio of IR peak intensities for sulfate to bisulfate increases as the applied potential is made more negative. In sulfuric acid, surface IR spectra indicate that adsorbed sulfate is favored at more positive potentials, while adsorbed bisulfate is prevalent at more negative voltages; also, a potential-dependent reorientation of water is observed in the spectra. IR spectroelectrochemical data from a sulfuric acid system containing copper sulfate indicate that adsorbed sulfate is present on gold at more positive potentials, and its coverage increases when underpotentially deposited (UPD) copper is present on the gold substrate surface. When the applied potential is sufficiently negative to effect full discharge of UPD copper, IR spectroelectrochemistry shows a loss of adsorbed sulfate and an increase in surface bisulfate species, with a concomitant reorientation of adsorbed water molecules. The results are explained in terms of surface electrostatic considerations during UPD of copper, and also in terms of potential-dependent pH changes at the interface. To our knowledge, this is the first reported infrared spectroelectrochemical study of interfacial changes occurring during metal underpotential deposition processes.

INTRODUCTION

In recent years infrared (IR) spectroelectrochemistry has been shown to be a valuable tool for investigations of the interactions of adsorbates with electrode surfaces.[1-4] For example, through IR spectroelectrochemical studies it has been demonstrated that adsorbed cations (as well as anions) may influence the potential-dependent behavior of coadsorbed species such as specifically adsorbed thiocyanate[5] and carbon monoxide.[6] Apart from double-layer studies, surface IR spectroelectrochemistry has proven to be extremely useful for examining mechanisms of electrode reactions,[1-4] since reaction intermediates at surfaces can be identified and characterized. By using IR spectroscopic techniques in combination with electrochemical systems, it is possible to investigate the nature of adsorbate bonding characteristics and potential-dependent orientational changes, as well as surface dynamics.[7-9] Also, detailed mechanistic information regarding electrode-mediated reactions can be obtained by using IR spectroelectrochemistry to monitor electrogenerated species in solution.[10]

The underpotential deposition (UPD) of foreign metals on electrode surfaces is an electrochemical phenomenon wherein an adlayer (or more) of certain metal species in solution may be reversibly and reproducibly deposited onto a substrate electrode surface prior to bulk metal deposition.[11,12] Surface-sensitive spectroscopic (and other interfacial) probes provide a means to study the effects of UPD on interfacial electrochemistry.[13-16] The work presented here utilizes the surface sensitivity of IR spectroelectrochemistry to explore how copper UPD affects the adsorption of sulfate and bisulfate on gold surfaces. To our knowledge, infrared spectroelectrochemistry has not

been used previously to investigate interfacial changes that occur as a result of metal underpotential deposition.

ADSORPTION OF SULFATE AND BISULFATE ON ELECTRODES

The coadsorption of bisulfate and sulfate on polycrystalline platinum surfaces has been the subject of several detailed IR spectroscopic studies.[17-20] A recent electrochemical study of bisulfate and sulfate adsorption on Pt(111),[21] and optical second-harmonic generation (SHG) studies of sulfate/bisulfate adsorption on polycrystalline silver[22] and platinum,[23] have also been published. Elsewhere, the behavior of bisulfate and sulfate ions on gold surfaces has been studied by voltammetry in potassium sulfate[24] and sodium sulfate[25] solutions, as well as in sulfuric acid.[24-26] An ex situ study employing Auger electron spectroscopy (AES), low-energy electron diffraction (LEED), and reflection high-energy electron diffraction (RHEED) of Au(111) surfaces following emersion of the electrode from sulfuric acid solutions has also been reported.[27] In this study,[27] it was reported that the sulfate AES peak intensity increased almost linearly with potential, and an ordered two-dimensional overlayer structure of sulfuric acid was demonstrated by LEED and RHEED regardless of the emersion potential between -0.2 and +0.6 V vs. Ag/AgCl. Adsorption of sulfate on gold electrodes has also been explored using the piezoelectric response of gold surfaces to aqueous sulfate solutions with changing potential.[25,28] The results of many of these investigations show that the detailed nature of sulfate and bisulfate adsorption is a strong function of the solution pH and the electrode potential, among other factors.

It is known that sulfate and bisulfate species may become specifically

adsorbed on gold surfaces, with the following anion adsorbability order for halides and sulfate/bisulfate: $F^- < HSO_4^- < SO_4^{2-} < Cl^- < Br^- < I^-$.[24] This order indicates that the presence of halide solution contaminants could affect the ability of sulfate/bisulfate to specifically adsorb on gold, and could also alter the orientation of surface sulfate species. In addition to the adsorbability order above, sulfate and bisulfate adsorption is probably controlled by slower adsorption kinetics than halides demonstrate under the same conditions. This conclusion is reached because sulfate/bisulfate adsorption is dependent upon potential sweep rates; this phenomenon is not observed for the halides.[24]

Previous electrochemical investigations of the sulfate/bisulfate system[24-26] have provided an understanding of the solution and surface conditions that influence sulfate and bisulfate adsorption, but have been largely insensitive to the differences in behavior of sulfate and bisulfate on the surface. While this earlier work showed that changing solution conditions alter the total relative surface concentrations of sulfate or bisulfate within a system, the relative surface concentrations of these two species were largely left to speculation. Infrared peak assignments, used earlier in the work with sulfate and bisulfate on platinum,[17-20] demonstrate that it is possible to differentiate between surface sulfate and bisulfate species by spectroelectrochemical means. Thus, it should be possible to gain a great deal of knowledge regarding sulfate/bisulfate adsorption on gold through the use of surface-sensitive IR techniques. In this paper we report the results of monitoring the potential-dependent surface behavior of sulfate and bisulfate anions, using IR spectroelectrochemistry as a surface probe.

UNDERPOTENTIAL DEPOSITION OF COPPER ON GOLD

The underpotential deposition (UPD) of copper on gold electrodes has been studied by a number of methods, including cyclic voltammetry,[13-15,29] surface-extended X-ray absorption fine structure (SEXAFS),[30,31] scanning tunneling microscopy (STM),[32,33] ex situ techniques (LEED, RHEED, and AES),[15] and AC impedance.[13,34] Further studies of the sulfate/bisulfate system employing radiotracer methods,[35] SHG,[36,37] the quartz crystal microbalance (QCM)[37,38] and X-ray absorption spectroscopy (XAS)[39] have also been conducted on both polycrystalline and single-crystal gold surfaces. Interpretation of the results from these studies has led to an understanding of the nature of the UPD copper adlayer on gold surfaces, and the determination that copper UPD does not result in alloy formation,[40] as was thought from earlier studies.[41] SEXAFS data from UPD copper monolayers on Au(111) electrodes in sulfuric acid electrolyte have allowed for the observation of oxygen associated with UPD copper atoms.[30,31] The source of this oxygen was attributed to either adsorbed sulfate/bisulfate or surface water.

While a reasonable understanding of the copper UPD on gold system is available, none of the techniques listed above have allowed for a detailed examination of the response of the electrolyte ions to the potential-induced changes occurring at the electrode surface. Radiotracer experiments,[35,42] which do indeed provide data on electrolyte ion behavior in a thin-layer cell, cannot differentiate between surface and solution species. Furthermore, the radiotracer technique does not allow for the determination of the orientation of adsorbed ions, and does not provide information on the behavior of surface water. SEXAFS studies do not reveal the source of the surface oxygen that is

associated with UPD copper atoms, i.e., whether the oxygen atom comes from H_2O or electrolyte anion/dianion. Voltammetric data suggest that faster kinetics are associated with the formation of submonolayers of Cu on polycrystalline gold in the presence of sulfate electrolyte, which is strongly adsorbed, vs. the case of perchlorate electrolyte, which adsorbs only weakly.[14] However, the precise behavior (i.e., coverage, orientation, etc.) of sulfate and water near the surface that leads to voltammetric differences between electrolyte ions cannot be determined from conventional electrochemical data. IR spectroelectrochemical data, on the other hand, may provide detailed information on the adsorption of both sulfate and bisulfate ions, as well as water, as a function of electrode potential. To date, neither the sulfate/bisulfate system on gold, nor copper UPD on gold in sulfuric acid, have been studied by IR spectroelectrochemical techniques. Under optimum conditions, surface-sensitive potential-dependent infrared (PDIR[43]) spectroscopy offers a number of advantages over other interfacial probes in that it can provide information on the identities, relative abundances, and orientations of adsorbed species. Using PDIR methods, a thorough investigation of surface sulfate/bisulfate electrolyte involvement in the Cu UPD process on gold will be described herein. The results from the UPD experiments will be compared with results from this electrolyte system in the absence of copper UPD. This study represents the first known use of in situ infrared spectroscopic techniques to probe interfacial changes that occur during UPD processes on electrode surfaces. This interfacial IR probe can be used to complement other surface-sensitive probes such as those mentioned previously (e.g., STM, SEXAFS, QCM, etc.).

EXPERIMENTAL

Infrared spectroscopic measurements were conducted by using an electrode potential modulation method combined with a Fourier transform IR spectrometer (IBM Instruments IR/98); the methodology has been described in detail previously.[1,2] A liquid nitrogen-cooled mercury-cadmium-telluride (MCT) detector (Infrared Associates) with its D^* maximum at ca. 1200 cm^{-1} was used throughout the study. The potential of the Au electrode (with respect to the reference electrode) was switched between reference (base) and sample potentials every 100 interferometer scans. A reference potential of +0.80 V vs. Ag/AgCl was chosen to facilitate comparisons with other studies of copper UPD on Au in sulfate electrolyte. All spectra reported here are difference spectra between the applied potentials indicated and the reference spectrum, unless otherwise noted. The potential modulation method was employed in order to keep the gold surface clean during the IR measurements. Typically 400 interferometer scans at the reference and sample potentials were collected with 4 cm^{-1} resolution to provide adequate signal/noise ratios.

A similar thin-layer spectroelectrochemical cell to the one used here has been described elsewhere,[44,45] except that the cell used in these experiments had a Kel-F® (rather than glass) cell body and piston. The cell was fitted with a ZnSe window (Spectra-Tech) with 20° bevelled edges at the front. The angle of incidence in the reflection measurements was roughly 70°. A smooth polycrystalline gold electrode (Johnson-Matthey), 25 mm diameter, 99.9985% purity, was used as the working electrode. A groove around the circumference of the gold electrode was added onto one side of the electrode disc to make the electrode to fit into a specially designed, o-ring sealed

Kel-F® piston. The piston allowed for electrical contact to be made with the gold electrode while sealing the contact from electrolyte solution. No solder or spot-welded joints were necessary. The groove reduced the effective diameter of the electrode to approximately 23 mm. The gold electrode was polished successively by 1, 0.3, and 0.05 μm alumina polishing powder (Buehler). Both the spectroelectrochemical cell and gold electrode were thoroughly cleaned in concentrated sulfuric acid (Vycor, doubly distilled) and rinsed exhaustively with 18 MΩ resistivity water (Barnstead Nanaopure system) before each experiment.

An Ag/AgCl (3 M KCl) reference electrode (Microelectrodes, Inc.) was placed in the main cell via a feedthrough near the front of the cell. All measurements were conducted at room temperature: 23 ± 1 °C. The cell was deaerated by bubbling ultrapure nitrogen (99.99%, Air Products) through a sealable cell port prior to the start of each experiment. Sulfate solutions were prepared by using Nanopure 18 MΩ water and doubly distilled sulfuric acid and/or sodium sulfate (99+%, Aldrich). Copper sulfate (Aldrich) was reagent grade and used as received. For the copper UPD on gold experiments, a 0.5 M H_2SO_4 solution containing 5 mM $CuSO_4$ was prepared. After collection of cyclic voltammograms, the gold electrode was pushed up against the ZnSe window for collection of PDIR spectra. The cell voltammetry was checked before and after PDIR spectroscopic studies to ensure that the electrode surface remained clean during the course of an experiment. Cyclic voltammograms (both in the presence and absence of copper) were similar in appearance to those reported previously in sulfate media,[25,37] and are indicative of well-behaved electrochemistry.

RESULTS AND DISCUSSION

SOLUTION CONDITIONS

The solution composition should play an important role in determining the ultimate surface sulfate interactions that are observed in an electrochemical system. The relative solution concentrations of sulfate and bisulfate ions are affected by the pH. Ratios of sulfate to bisulfate for various solution compositions have been calculated using the dissociation constant of the bisulfate anion,[46] assuming the activity coefficients $a_+ = a_- = a_\pm$, and are listed in Table I. Experimentally determined absolute concentrations of sulfate and bisulfate have been measured by Raman spectroscopy in sulfuric acid solutions,[47-50] but the relative concentrations of these ions in solution will be adequate for discussion here. In the case of copper UPD on gold, the insolubility of $CuSO_4$ at higher pH requires the use of acidic solution conditions; hence data from systems containing copper are obtained in 0.5 M H_2SO_4.

SURFACE IR SPECTROELECTROCHEMISTRY OF SULFATE AND BISULFATE ON GOLD

In order to interpret PDIR spectra of sulfate and bisulfate species obtained during copper UPD on gold studies (which will be discussed later), it is useful to investigate the IR spectroelectrochemistry of the sulfate/bisulfate system in the absence of copper. Figures 1 and 2 show the difference spectra collected from a polycrystalline gold surface when the reference potential is ratioed against the sample potential for solutions of 0.5 M Na_2SO_4 and 0.5 M

H_2SO_4, respectively. Positive peaks in the spectra arise from species prevalent at the reference potential, while negative peaks are due to species present at the sample voltage.[1] Verification of the observed spectral features as being due to surface species was accomplished by comparing s- and p-polarized spectra.[1,2] No peaks appeared in the spectrum obtained with s-polarized radiation, indicating that the peaks in Figures 1 and 2 arise from species at the electrode surface. The surface attributes of the observed peaks have been established in earlier studies of the sulfate/bisulfate system within the double-layer region on platinum.[18] By keeping within the double-layer potential region, spectral complications arising from faradaic processes[51] and the migration of solution electrolyte species (into or out of) the thin layer[52] have been minimized. The observed peaks in the PDIR spectra (Figures 1 and 2) also demonstrate slight potential-dependent frequency shifts, which offers further evidence that the observed spectral features are due to surface species.

Examination of IR difference spectra from Na_2SO_4 and H_2SO_4 systems on polycrystalline gold (Figures 1 and 2, respectively) reveal several peaks in the 850 to 1250 cm^{-1} range, with four main peaks appearing at approximately 900, 1050, 1100, and 1200 cm^{-1}. These peaks have been assigned to vibrations of surface bisulfate and sulfate ions,[17-20,53-55] and are summarized in Table II. Figure 2 also shows a large bipolar band centered around ca. 1600 cm^{-1}, which is attributed to the bending mode of interfacial water molecules. The most striking features in the data are the differences observed between the signs of the sulfate and bisulfate peaks in the two systems (Figures 1 and 2). The data of Figure 1 show a strong positive peak at ca. 1100 cm^{-1}, which is attributed to sulfate on the electrode surface, and negative peaks at ca.

1200, 1050, and 900 cm^{-1}, which are assigned to surface bisulfate. The data presented in Figure 2 show an opposite trend from that seen in Figure 1, i.e., positive peaks are observed at ca. 1200, 1050, and 900 cm^{-1} (due to surface bisulfate), and a strong negative peak appears at ca. 1100 cm^{-1} (due to surface sulfate). Strong water bands near ca. 1600 cm^{-1} are also observed in the sulfuric acid system (Figure 2), while no significant water bands in this wavenumber region appeared in the sodium sulfate case (Figure 1). These results indicate that in sodium sulfate solution there is more bisulfate on the surface with increasing potential, while in sulfuric acid there is more sulfate adsorption occurring with increasing potential. In other words, the sulfate vs. bisulfate behavior is reversed depending upon the identity of the predominant cation in solution (H^+ or Na^+). Also apparent from the IR spectroelectrochemical data is the presence of surface water in solutions of high acidity (Figure 2); surface water is possibly absent, or (most likely) is not affected by potential changes in more neutral solution (Figure 1). Thus the solution pH influences solvent, as well as electrolyte, adsorption characteristics. The spectroscopic results from acidic solutions are similar to what has been observed for the same solutions on platinum surfaces.[18]

In order to extract more precise information from the data presented in Figures 1 and 2, a fitting method involving the summation of model Gaussian peaks was used to model the experimental PDIR data. This method has been employed previously with similar data from adsorbed thiocyanate in an effort to simulate difference spectra that yield overlapping peaks of opposite sign.[56] Modeling methods of this kind are also useful for alleviating problems in the interpretation of difference spectra, especially in instances where the reference spectrum is not a flat baseline and there are overlapping

peaks.[57] For the sake of simplicity, a single peak width was assigned to each Gaussian peak regardless of the applied potential, i.e., we assume no potential-dependent change in peak widths. Peak amplitudes and peak positions are different for each Gaussian in every fit of experimental data, and were varied to obtain a least squares fit for each spectrum that was modeled. In modeling IR spectroelectrochemical data obtained from 0.5 M Na_2SO_4, three Gaussian peaks (with frequency maxima at ca. 1200, 1100, and 1050 cm^{-1}) were used. For fits of PDIR data from 0.5 M H_2SO_4 solution, only two Gaussians (peak frequencies ca. 1200 and 1100 cm^{-1}) were employed, since the 1050 cm^{-1} was not prominent in the original spectrum.

The results of the fit for PDIR spectra obtained in 0.5 M Na_2SO_4 and 0.5 M H_2SO_4 are shown in Figures 3 and 4, respectively. Figures 5a and 5b show examples of plots of experimental results along with the residuals (differences between the experimental and fitted data) for the above sodium sulfate and sulfuric acid solutions, respectively. While the three-Gaussian fit for the sodium sulfate solution (Figure 5a) has fairly random, small residuals, the residuals for the case of sulfuric acid (Figure 5b) reflect the presence of a weak feature at ~1050 cm^{-1} which was not easily observed in the original unfitted PDIR data. By modeling experimental infrared data in this fashion, it becomes possible to assign more accurate peak parameters (i.e., peak frequency, width and intensity) to overlapping peaks in difference spectra.

Peak positions determined from the fitted data from 0.5 M Na_2SO_4 or H_2SO_4 are shown in Figures 6a and 6b for the ~1100 cm^{-1} (sulfate) and ~1200 cm^{-1} (bisulfate) peaks, respectively. It is apparent from the plots (Figure 6) that the peak frequency for both the sulfate and bisulfate peaks is greater

under more acidic conditions. The reasons for these differences in peak frequencies (for adsorbed sulfate and bisulfate species) may arise from a variety of factors, including differences in orientation, coverage, degree of hydrogen bonding, etc. Neither the sulfate nor bisulfate peaks show substantial potential-dependent frequency shifts, if compared to frequency shifts observed for adsorbed CO and pseudohalide species (which are significantly higher).[1] This observation may be due to the unavailability of polarizable electrons in single bonds of sulfate and bisulfate species, which leads to a lower Stark tuning rate than for double- and triple-bonded adsorbates such as CO_{ads} and CN^-_{ads}. As the applied potential is made more positive, slight shifts to higher frequency are observed for adsorbed sulfate and bisulfate species in Na_2SO_4 and H_2SO_4 solutions, with the exception of the sulfate peak (~1200 cm^{-1}) in sulfuric acid solution (Figure 6). This peak shows a frequency decrease with increases in potential above ca. -0.1 V (Figure 6b), and is probably due to increasing sulfate coverage (and therefore greater adsorbate-adsorbate coupling) at higher potentials. This contention is consistent with capacity and electrochemical quartz crystal microbalance (EQCM) data on polycrystalline gold, which suggest higher sulfate coverages at more positive potentials in sulfuric acid.[25]

Peak intensities of adsorbed sulfate and bisulfate species, unlike peak positions, show more pronounced dependencies on potential (Figure 7). It is clear from these results that the interfacial pH has a profound influence on the relative identities and coverages of adsorbed sulfate species as the potential is altered within the double layer region. The sulfate peak at ~1100 cm^{-1} is generally much more intense in the acidic system (Figure 2) than in the more basic system (Figure 1). This may be ascribed to the existence of

a contact-adsorbed sulfate species in acid, as opposed to a solvent-separated interfacial sulfate species in the more basic system, which results in a higher band intensity due to an enhancement effect.[58] Interfacial bisulfate species are thought to be solvent-separated in all cases, since no drastic intensity changes (comparing Figures 1 and 2) are noted for bisulfate spectral bands. Fitted peak intensity vs. potential data for 0.5 M Na_2SO_4 and 0.5 M H_2SO_4 are shown in Figures 7a,b; note the differences in scale for the two cases. The trends in the fitted data for the ~1200 cm^{-1} (bisulfate asymmetric stretch) peak (Figure 7) suggest that for predominantly acidic solutions, HSO_4^- is lost from the surface as the potential is increased. On the other hand, under more neutral conditions, there is a small increase in bisulfate adsorption with increasing potential, followed by a weak desorption trend. The ~900 cm^{-1} (S-(OH) stretching) peak position follows the behavior of the other (~1200 cm^{-1}) bisulfate peak. These trends were less obvious in unfitted intensity vs. potential data, and again demonstrate the importance of fitting difference infrared spectra.

The intensity vs. potential trends for the ~1100 cm^{-1} peak (asymmetric sulfate vibration), illustrated in Figure 7, are opposite the trends observed for bisulfate. For more acidic solutions (0.5 M H_2SO_4), the amount of adsorbed sulfate on the gold surface appears to increase dramatically with potential above approximately -0.1 V. However, the amount of adsorbed sulfate, indicated by the intensity of the ~1100 cm^{-1} peak, changes less with potential for the more neutral solutions. In more neutral conditions (0.5 M Na_2SO_4), adsorption of sulfate decreases by a similar degree to the increases in adsorption that are observed for bisulfate, as indicated by the intensities of the ~1200 and ~900 cm^{-1} peaks. So at more positive applied potentials,

sulfate adsorption appears to be favored in more acidic media, while bisulfate adsorption predominates in more neutral solutions.

The reasons for the differences in adsorption behavior between acidic (i.e., 0.5 M H_2SO_4) and neutral (e.g., 0.5 M Na_2SO_4) cases do not appear to be due to significant differences in the gold surface charge. While we did not determine the potentials of zero charge (pzc's) for the solutions under study here, pzc's of gold surfaces under similar solution conditions have been reported.[59,60] The pzc of polycrystalline gold in 1 M H_2SO_4 has been determined to be +0.070 V[59] (vs. the reversible hydrogen electrode, or RHE), and the pzc for this surface in 0.1 M Na_2SO_4 has been reported (for solutions of pH 2-8) to be +0.12 V[60] (vs. RHE). As these values do not vary widely, it is probable that there is no large change in the pzc with the changes in solution conditions used in the experiments. Also, since the experiments here were conducted within the double layer potential region, effects due to hydrogen adsorption and/or oxide formation should not be important. Hence, other influences besides changes in surface charge and hydride or oxide formation must be responsible for the observed potential-dependent adsorption behavior of sulfate and bisulfate in the solutions investigated here. It seems clear that the solution pH (and therefore the pH of the interfacial region) is responsible for the above spectroelectrochemical observations. Influences of H^+ concentration on adsorption have been noted before in PDIR studies, for example in the adsorption behavior of the acetate/acetic acid system[52,61] and surface cyanide species.[51]

Differences in H^+ concentration would have the most profound effect on the surface behavior of sulfate and bisulfate anions if an equilibrium relation between surface species is more dominant than the equilibrium between

surface and solution species. A model for this type of behavior was proposed previously to explain sulfate and bisulfate adsorption on platinum.[18] Consider the dissociation of adsorbed bisulfate species to sulfate plus an interfacial proton:

$$(HSO_4^-)_{ads} = (H^+)_{int} + (SO_4^{2-})_{ads} ,$$

so that

$$K_{ads} = \{[(H^+)_{int}] \times [(SO_4^{2-})_{ads}]\}/[(HSO_4^-)_{ads}] .$$

A high interfacial H^+ concentration would tend to drive the above equilibrium to favor surface bisulfate. Applying the second expression to the case where sodium cation (and not H^+) is predominant at the surface, it is apparent that the sodium concentration should not significantly affect the relative surface concentrations of SO_4^{2-} or HSO_4^-. Alternatively, at lower pH, the higher concentration of H^+ at the interface should have a substantial influence on K_{ads}, especially at less positive potentials where the proton concentration in the interfacial region is high. For systems with low H^+ concentrations (e.g., 0.5 M Na_2SO_4), this model predicts only a small change in sulfate and bisulfate peak intensities as the potential is changed, while for more acidic solutions (e.g., 0.5 M H_2SO_4), the surface equilibrium model predicts a more pronounced peak intensity change with potential. These predictions are reflected in the data of Figure 7, which reveal greater potential-induced intensity changes for the highly acidic system (Figure 7b) vs. more neutral solution (Figure 7a). Also (in the acidic system) as expected from the model,

when the applied potential is made more positive, H^+ leaves the surface, the sulfate coverage increases, and the bisulfate coverage decreases. The above equilibrium model is consistent with the data of Figures 7, which illustrate (for neutral as well as for acidic systems) that as a bisulfate peak (at ~1200, or ~900 cm^{-1}) gains (loses) intensity, the sulfate peak (at ~1100 cm^{-1}) goes in the opposite direction, with a corresponding intensity decrease (increase). It is necessary to employ the above surface equilibrium model in an effort to explain our PDIR data, for the concentration ratios presented in Table I do not account for the coexistence of surface sulfate and bisulfate species in both acidic and neutral media.

ADSORBED WATER ON GOLD

It is of interest to consider the behavior of the ~1600 cm^{-1} bending water vibration in the PDIR spectra from highly acidic solutions such as 0.5 M H_2SO_4 (Figure 2). This band was not observed in PDIR data from more neutral aqueous media, e.g., 0.5 M Na_2SO_4 (Figure 1). As the applied potential is made more negative, the peak frequency shifts from lower to higher wavenumbers. The implication is that in acidic media, adsorbed water reorients when the potential is changed within the double layer regime. Surface water is oriented with its oxygen atom toward the surface at more positive potentials, and flips over as the potential is made more negative to become oriented with the hydrogen atoms toward the surface. Since there is less strain on the bending vibrational mode if the oxygen of the water molecule is oriented toward the surface, the peak frequency is lower than for an oscillation where the hydrogens are near the surface. While it is probable

that adsorbed water is also present in the case of neutral solution, no significant peaks appear in the ~1600 cm^{-1} region in the difference IR spectroelectrochemical data (Figure 1). Hence, there is apparently no potential-induced reorientation of adsorbed water in the more neutral system. These results show that an increase in the interfacial pH not only affects the adsorption behavior of sulfate and bisulfate species, but also influences the behavior of water in the interfacial region. A higher interfacial H^+ concentration at more negative potentials in a system where protons are readily available would result in higher local concentrations of hydronium ion. Protonation of surface water would then result in a reorientation from oxygen-down to hydrogens-down.

COPPER UNDERPOTENTIAL DEPOSITION ON GOLD IN SULFURIC ACID

From voltammetric studies, it is known that bulk copper is deposited cathodically (from Cu^{2+} dissolved in sulfate solution) onto gold surfaces at voltages negative of approximately 0.05 V vs. Ag/AgCl.[13-15,37] Copper UPD on both polycrystalline and single-crystal gold surfaces reveals two UPD waves; these waves are much narrower and more well-defined on single-crystal (e.g., Au(111))[38,62] surfaces than they are on polycrystalline surfaces.[37] Also, on polycrystalline gold, the second UPD peak and the current peak due to bulk copper electrodeposition are not nearly as well-resolved as on single-crystal gold surfaces.[37] Coulometric measurements on both polycrystalline gold and Au(111) suggest that the first copper UPD peak corresponds to a $Cu^{2+} \rightarrow Cu^{+}$ reduction, while the second UPD peak is due to $Cu^{+} \rightarrow Cu^{o}$.[38] This is consistent with interpretations from XAS measurements on single-crystal surfaces, which

point to the existence of a Cu^+ adlayer between the first and second UPD peaks.[39] However, there is conflicting evidence from LEED,[15] STM,[32,33] and other voltammetric[63] and EQCM[37,64] studies which suggest that the charge of the initially deposited copper adlayer is less than +1. Coulometric data are not always reliable, since partial charge transfer may occur due to ionic adsorption.[15,63] So the assigned charge of the initially deposited copper adlayer remains an open question. However, there is no doubt that this UPD adlayer is not fully discharged, and that full discharge to Cu^o does not occur until further negative potentials are applied. Whatever the charge of the first Cu UPD adlayer, it is emphasized that a significant amount of positive charge is retained. For arguments presented here, an assignation of +1 charge to the first UPD adlayer will not affect our interpretation of spectral changes that result from influences of the changing surface charge.

The cyclic voltammetry of the $CuSO_4$ + H_2SO_4 system on vapor-deposited polycrystalline gold has been published.[37] On this gold surface, during a negative scan from a starting potential of +0.8 V (vs. Ag/AgCl), the first and second UPD peaks appear at ~+0.20 and ~+0.05 V, respectively. On the return positive scan, the corresponding UPD stripping peaks are observed at ~+0.10 and ~+0.22 V for $Cu^o \rightarrow Cu^+$ and $Cu^+ \rightarrow Cu^{2+}$, respectively. It is emphasized that the UPD waves on polycrystalline gold are much broader and ill-defined than the corresponding waves on single-crystal gold surfaces. Infrared spectroelectrochemical data were obtained from this system at applied potentials between +0.8 V and -0.05 V, as described below.

The spectra shown in Figure 8 are PDIR results collected during UPD of copper on polycrystalline gold from a 0.5 M H_2SO_4 + 5 mM $CuSO_4$ solution. These spectra illustrate that copper UPD has a strong influence on the

interfacial behavior of sulfate, bisulfate, and water. Let us first examine the PDIR spectra obtained within the potential region where Cu^{o} UPD occurs (e.g., +0.0 and -0.05 V, Figure 8). These spectra are very similar in appearance to those collected from 0.5 M H_2SO_4 on gold with no copper present (Figure 2). However, PDIR spectra taken within the Cu^{+} UPD potential regime (e.g., +0.29 and +0.2 V, Figure 8) are similar to the difference spectra recorded from 0.5 M Na_2SO_4 on gold (Figure 1), where no copper is present. The IR spectroelectrochemical data shown in Figure 8 illustrate that significant interfacial changes occur during copper UPD. The sulfate peak at ~1100 cm^{-1} first gains intensity within the realm of Cu^{+} UPD, and then significantly loses intensity as underpotentially deposited Cu^{+} is converted to Cu^{o}. Bisulfate peaks at ~1200, 1050, and 900 cm^{-1}, as before in systems where no copper was present, go in the opposite direction to sulfate peaks. During Cu^{+} UPD, bisulfate peaks decrease in intensity, and then grow in intensity as UPD Cu^{o} is formed electrochemically. The bipolar water band near ~1600 cm^{-1} also appears when Cu^{o} is formed. Such detail regarding the interfacial behavior of electrolyte and solvent during UPD processes has not been revealed by other surface probes, and shows the utility of IR spectroelectrochemistry for UPD studies.

The implications of the results shown in Figure 8 are intriguing. When UPD Cu^{+} is present on the gold substrate surface, the interfacial pH is similar to that for 0.5 M Na_2SO_4 solution. Hence, the concentration of H^{+} near the interface is small, and adsorbed sulfate predominates over surface bisulfate species, as suggested by the PDIR spectra (compare Figures 1 and 8). On the other hand, when UPD Cu^{o} is formed, the interfacial pH becomes similar to that for 0.5 M H_2SO_4, and now bisulfate adsorption is favored; also,

surface water undergoes a reorientation (with respect to the reference voltage at +0.8 V) such as that seen earlier (Figure 2). A positively charged UPD copper adlayer (Cu^{+1}) would disfavor the presence of H^+ near the surface, even in a highly acidic medium such as that here. This situation would then favor adsorption of sulfate species on the UPD adlayer, as was seen at less positive potentials in the case of a neutral sulfate electrolyte on a gold surface (Figure 1). However, a fully discharged surface layer of copper, such as Cu^0 on gold, would not expel H^+ from the interface, especially at potentials negative of the pzc. Hence bisulfate species will be prevalent on the fully discharged UPD copper surface; this is reflected in the PDIR spectra (compare Figures 2 and 8). Concurrent with these observations (Figure 8) is the reorientation of interfacial water (from oxygen down to hydrogens down) as a result of Cu^0 formation; this result is virtually identical to the behavior in 0.5 M H_2SO_4 on gold (Figure 2). The interfacial pH is thus a function of the surface charge, not only of the substrate electrode, but also of the UPD adlayer. The interfacial H^+ concentration therefore influences the relative surface concentrations of polyprotic electrolyte species, and also affects the adsorption behavior of surface water molecules by causing a corresponding increase in the local hydronium ion concentration.

SUMMARY

Based on the IR spectroelectrochemical results from 0.5 M Na_2SO_4, 0.5 M H_2SO_4, and 5 mM $CuSO_4$ in 0.5 M H_2SO_4 on polycrystalline gold, a general model of the interface can be postulated as a function of pH and applied potential

(Figure 9). In sodium sulfate on bare gold, there is co-adsorption of sulfate and bisulfate at applied potentials within the double-layer region. As the voltage is made more negative, the sulfate coverage increases and the bisulfate coverage decreases. However, in acid medium, we have the opposite scenario, i.e., as the potential is made more negative, the sulfate coverage decreases while the coverage of bisulfate increases. Also, at more positive potentials in H_2SO_4, there appears to be higher coverage of sulfate vs. bisulfate. Furthermore, reorientation of surface water occurs in sulfuric acid, which is not seen in the sodium sulfate case. Finally, in a system where copper underpotential deposition (first UPD of Cu^+ and subsequently full discharge to Cu^o) occurs, the behaviors of sulfate and bisulfate species demonstrate attributes of both sodium sulfate and sulfuric acid systems. At more positive applied potentials, there exists predominately adsorbed sulfate, although there remains some surface bisulfate. As the potential is made more negative and a Cu^+ UPD layer is present on gold, the sulfate coverage increases while the amount of surface bisulfate decreases. Then when UPD copper is fully discharged (to UPD Cu^o), sulfate becomes desorbed and the bisulfate coverage increases. This change in the ratio of sulfate/bisulfate at the surface during conversion of Cu^+ to Cu^o is accompanied by a concomitant reorientation of surface water from oxygen-down to hydrogens-down.

The intensities of bisulfate IR peaks in the PDIR data (Figures 1, 2 and 8) suggest that bisulfate which is associated with the electrode surface is not contact adsorbed on the electrode surface; rather, surface water molecules are present between surface bisulfate and the electrode itself (Figure 9). On the other hand, observations of significantly higher peak intensities for surface sulfate under certain conditions suggest that this species may become

contact adsorbed on the gold surface at more positive potentials (Figure 2), and also on a UPD copper adlayer when UPD occurs (Figure 8). When contact adsorbed sulfate (Figure 9) is removed from the surface, e.g., at potentials favoring fully discharged UPD copper or at voltages negative of the gold pzc on a bare electrode, surface water molecules undergo reorientation (Figure 2, 8). This reorientation of $(H_2O)_{ads}$ (described above) is not observed in sodium sulfate; nor does it appear, based on the observation of lower sulfate peak intensities compared to the acidic case (Figures 1 and 2), that surface sulfate is contact adsorbed on the gold surface in Na_2SO_4 (Figure 9).

The PDIR results from polycrystalline gold, obtained in acid medium (0.5 M H_2SO_4), can be rationalized in the following manner. At more positive potentials, the interfacial H^+ concentration is low, and adsorption of the more highly negatively-charged species (i.e., sulfate) is favored. Also, the more electron-rich portion of surface water (i.e., oxygen) is oriented toward the surface. Now as the potential is made more negative (to applied voltages negative of the gold pzc), the surface pH decreases (concentration of H^+ in the interface increases). This results in protonation of surface sulfate to form surface bisulfate, desorption of surface sulfate, and reorientation of water so that the more electron-poor regions of the water molecule, i.e., hydrogens, are toward the electrode surface. If the potential is made sufficiently negative there is an overall decrease in the total coverage of surface sulfate/bisulfate; this is consistent with EQCM studies on polycrystalline gold surfaces, which show an overall mass decrease at more negative potentials.[25]

We may explain the implications of the PDIR data obtained from 0.5 M Na_2SO_4 on gold (Figure 1) in the following way. To reiterate, the PDIR

spectra indicate that the concentration of surface sulfate increases, and the amount of bisulfate at the surface decreases, as the potential is made more negative. At first glance this appears counter-intuitive, for the amount of a surface species of higher negative charge (SO_4^{2-}) is increasing at further negative voltages, while the coverage of an adsorbate of lower negative charge (HSO_4^-) is decreasing as the applied potential becomes less positive. However, we must take into account the fact that the amount of sodium ion at the interface is increasing as the voltage is made more negative. Since Na^+, rather than H^+, is the predominant cation in solution ($[H^+]$ is approximately 4 x 10^{-6} M, while $[Na^+]$ is ca. 1 M), more sodium ion must be attracted to the electrode surface at more negative voltages in order to maintain charge balance at the interface. This will serve to increase the interfacial pH as the potential is made more negative, thereby favoring the existence of surface sulfate (deprotonated form) over surface bisulfate (protonated from). While it is thought that adsorbed water exists at the surface (Figure 9), the PDIR results indicate no potential-dependent change in orientation of $(H_2O)_{ads}$.

The situation in 0.5 M H_2SO_4 when copper is present demonstrates some very interesting potential-dependent adsorption behavior on the part of the sulfate and bisulfate species. At further positive potentials the surface structure mimics that of sulfuric acid (no copper), which has already been discussed. That is, we have a predominance of adsorbed sulfate on the gold surface, and water is oriented oxygen-down. At potentials when UPD copper is present, the amount of adsorbed sulfate increases since the UPD copper adlayer is positively charged (Cu^+); this favors adsorption of the more negatively charged adsorbate. This interpretation is consistent with EQCM results on Au(111) surfaces that suggest adsorption of sulfate at more positive

potentials, and also during copper UPD.[38] The existence of a Cu^+ UPD adlayer upon which sulfate is contact adsorbed is also consistent with XAS studies on Au(111) that arrive at the same conclusions.[39] When a UPD copper adlayer is present (which is not fully discharged), surface water remains oxygen-down, since the more electron-rich portion of the water molecule will be attracted to a positively charged substrate surface. However, when the applied voltage is made sufficiently negative to induce full discharge of the UPD copper adlayer (Cu^o), the existence of a negative applied potential causes an increase in the interfacial concentration of H^+. This results in a loss in the amount of adsorbed sulfate and a gain in the concentration of surface bisulfate. Furthermore, surface water reorientation, which appears to be driven in part by the potential-dependent change in interfacial pH, occurs so that the more positive portion of the molecule is directed toward the substrate surface.

ACKNOWLEDGMENTS

We thank Drs. Joe Gordon and Larry Olsen for helpful discussions, and Bruce Hoenig and Gary Borges for invaluable technical assistance. This work was supported in part by the Office of Naval Research. K. A. acknowledges support from Research Corporation and the donors of the Petroleum Research Fund, administered by the American Chemical Society.

REFERENCES

1. Ashley, K.; Pons, S. Chem. Rev. 1988, 88, 673, and references therein.

2. Bewick, A.; Pons, S. In Advances in Infrared and Raman Spectroscopy; Clark, R. J. H.; Hester, R. E., Eds.; Wiley-Heyden: London, 1985, Vol. 12.

3. Seki, H. In Electrochemical Surface Science; Soriaga, M. P., Ed.; American Chemical Society: Washington, DC, 1988.

4. Stole, S. M.; Popenoe, D. D.; Porter, M. D. In Electrochemical Interfaces; Abruña, H. D., Ed.; VCH Publishers: New York, 1991.

5. Ashley, K.; Samant, M. G.; Seki, H.; Philpott, M. R. J. Electroanal. Chem. 1989, 270, 349.

6. Anderson, M. R.; Huang, J. J. Electroanal. Chem. 1991, 318, 335.

7. Ashley, K.; Weinert, F.; Samant, M. G.; Seki, H.; Philpott, M. R. J. Phys. Chem. 1991, 95, 7409.

8. Ashley, K.; Weinert, F.; Feldheim, D. L. Electrochim. Acta 1991, 36, 1863.

9. Ashley, K.; Lazaga, M.; Samant, M. G.; Seki, H.; Philpott, M. R. Surf. Sci. 1989, 219, L590.

10. Ashley, K. Talanta 1991, 38, 1209, and references therein.

11. Kolb, D. M. In Advances in Electrochemistry and Electrochemical Engineering; Gerischer, H., and Tobias, C. W., Eds.; Pergamon Press: New York, 1978; Vol. 11.

12. Kolb, D. M.; Przasnyski, M.; Gerischer, H. J. Electroanal. Chem. 1974, 54, 25.

13. Farmer, J. C. J. Electrochem. Soc. 1985, 132, 2640.

14. Xing, X.; Scherson, D. J. Electroanal. Chem. 1989, 270, 273.

15. Zei, M. S.; Quiao, G.; Lehmpfuhl, G.; Kolb, D. M. Ber. Bunsenges. Phys. Chem. 1987, 91, 349.

16. Melroy, O. R.; Kanazawa, K.; Gordon, J. G.; Buttry, D. Langmuir 1986, 2, 697.

17. Kunimatsu, K.; Samant, M. G.; Seki, H.; Philpott, M. R.; J. Electroanal. Chem. 1988, 243, 203.

18. Kunimatsu, K.; Samant, M. G.; Seki, H. J. Electroanal. Chem. 1989, 258, 163.

19. Kunimatsu, K.; Samant, M. G.; Seki, H. J. Electroanal. Chem. 1989, 272, 185.

20. Samant, M. G.; Kunimatsu, K.; Seki, H.; Philpott, M. R. J. Electroanal. Chem. 1990, 280, 391.

21. Faguy, P. W.; Marković, N.; Adžić, R. R.; Fierro, C. A.; Yeager, E. B. J. Electroanal. Chem. 1990, 289, 245.

22. Robinson, J. M.; Richmond, G. L. Electrochim. Acta 1989, 34, 1639.

23. Campbell, D. J.; Corn, R. M. J. Phys. Chem. 1988, 92, 5796.

24. Tucceri, R. I.; Posadas, D. J. Electroanal. Chem. 1985, 191, 387.

25. Stöckel, W.; Schumacher, R. Ber. Bunsenges. Phys. Chem. 1987, 91, 345.

26. Strbać, S.; Adžić, R. R. J. Electroanal. Chem. 1988, 249, 291.

27. Zei, M. S.; Scherson, D.; Lehmpfuhl, G.; Kolb, D. M. J. Electroanal. Chem. 1987, 229, 99.

28. Seo, M.; Jiang, X. C.; Sato, N. J. Electrochem. Soc. 1987, 134, 3094.

29. Angerstein-Kozlowska, H.; Conway, B. E.; Hamelin, A.; Stoicoviciu, L. Electrochim. Acta 1986, 31, 1051.

30. Melroy, O. R.; Samant, M. G.; Borges, G. L.; Gordon, J. G.; Blum, L.; White, J. H.; Albarelli, M. J.; McMillan, M.; Abruña, H. D. Langmuir 1988, 4, 728.

31. Blum, L.; Abruña, H. D.; White, J. H.; Gordon, J. G.; Borges, G. L.; Samant, M. G.; Melroy, O. R. J. Chem. Phys. 1986, 85, 6732.

32. Magnussen, O. M.; Hotlos, J.; Nichols, R. J.; Kolb, D. M.; Behm, R. J. Phys. Rev. Lett. 1990, 64, 2929.

33. Hachiya, T.; Honbo, H.; Itaya, K. J. Electroanal. Chem. 1991, 315, 275.

34. Jović, V. D.; Jović, B. M.; Parsons, R. J. Electroanal. Chem. 1990, 290, 257.

35. Horanyi, G.; Rizmayer, E.; Joo, P. J. Electroanal. Chem. 1985, 152, 211.

36. Bennahmias, M. J.; Lakkaraju, S.; Stone, B. M.; Ashley, K. J. Electroanal. Chem. 1990, 280, 429.

37. Lakkaraju, S.; Bennhamias, M. J.; Borges, G. L.; Gordon, J. G.; Lazaga, M.; Stone, B. M.; Ashley, K. Appl. Opt. 1990, 29, 4943.

38. Borges, G. L. M. S. Thesis, San Jose State University, 1992.

39. Tadjeddine, A.; Tourillon, G.; Guay, D. Electrochim. Acta 1991, 36, 1859.

40. Turner, D. J. J. Chem. Soc., Faraday Trans. 2 1972, 68, 643.

41. Van der Eerden, J.; Staikov, G.; Hashchiv, D.; Lorenz, W.; Budevski, E. Surf. Sci. 1979, 82, 364.

42. Zelenay, P.; Wieckowski, A. In Electrochemical Interfaces; Abruña, H. D., Ed.; VCH Publishers: New York, 1991.

43. Corrigan, D. S.; Weaver, M. J. J. Phys. Chem. 1986, 90, 5300.

44. Kunimatsu, K.; Golden, W. G.; Seki, H. Langmuir 1985, 1, 285.

45. Ashley, K. Spectroscopy 1990, 5(1), 22.

46. Pitzer, K. S.; Roy, R. N.; Silvester, L. F. J. Am. Chem. Soc. 1977, 99, 4930.

47. Irish, D. E.; Chen, H. J. Phys. Chem. 1970, 74, 3796.

48. Chen, H.; Irish, D. E. J. Phys. Chem. 1971, 75, 2672.

49. Turner, D. J. J. Chem. Soc., Faraday Trans. 1 1974, 70, 1346.

50. Balej, J.; Hanousek, F.; Pisarcik, M.; Sarka, K. J. Chem. Soc., Faraday Trans. 1 1984, 80, 521.

51. Paulissen, V. B.; Korzeniewski, C. J. Phys. Chem. 1992, 96, 4563.

52. Bae, I. T.; Scherson, D. A.; Yeager, E. B. Anal. Chem. 1990, 62, 45.

53. Nakamoto, K. Infrared and Raman Spectra of Inorganic and Coordination Compounds, 4th ed.; Wiley: New York, 1986, Ch. 3.

54. Dawson, B. S. W.; Irish, D. E.; Toogood, G. E. J. Phys. Chem. 1986, 90, 334.

55. Clarke, J. H. R.; Woodward, L. A. Trans. Faraday Soc. 1968, 64, 1041.

56. Parry, D. B.; Harris, J. M.; Ashley, K. Langmuir 1990, 6, 209.

57. Parry, D. B.; Samant, M. G.; Melroy, O. R. Appl. Spectrosc. 1991, 45, 999.

58. Korzeniewski, C.; Shirts, R. B.; Pons, S. J. Phys. Chem. 1985, 89, 2297.

59. Levin, E. D.; Rotinyan, A. L. Electrokhimiya 1972, 8, 240.

60. Bode, D. D., Jr.; Andersen, T. N.; Eyring, H. J. Phys. Chem. 1967, 71, 792.

61. Corrigan, D. S.; Krauskopf, E. K.; Rice, L. M.; Wieckowski, A.; Weaver, M. J. J. Phys. Chem. 1988, 92, 1596.

62. Kolb, D. M. Ber. Bunsenges. Phys. Chem. 1988, 92, 1175.

63. Leung, L. H.; Gregg, D. W.; Goodman, D. W. Chem. Phys. Lett. 1992, 188, 467.

64. Deakin, M. R.; Melroy, O. R. J. Electroanal. Chem. 1988, 239, 321.

Table I. Calculated sulfate/bisulfate concentration ratios for various solution compositions of sodium sulfate + sulfuric acid.

solution	sulfate conc./bisulfate conc.
0.5 M Na_2SO_4	1.2×10^5
0.5 M Na_2SO_4 + 0.01 M H_2SO_4	49
0.25 M Na_2SO_4 + 0.25 M H_2SO_4	0.15
0.5 M H_2SO_4	0.021

Table II. Assignments of vibrational mode frequencies for sulfate and bisulfate species.

Approximate Peak Frequency, cm^{-1}	Vibrational Mode
~1200	bisulfate asymmetric SO_3 stretch
~1100	sulfate asymmetric SO_3 stretch
~1050	bisulfate symmetric SO_3 stretch
~900	bisulfate S-(OH) stretch

FIGURE LEGENDS

Figure 1. PDIR spectra obtained from aqueous 0.5 M Na_2SO_4 on polycrystalline gold. The reference spectrum was obtained at +0.8 V vs. Ag/AgCl, and the sample spectra were obtained at the applied potentials shown in the figure.

Figure 2. PDIR spectra obtained from 0.5 M H_2SO_4 on polycrystalline gold. The reference potential was +0.8 V vs. Ag/AgCl, and sample voltages are as shown in the figure.

Figure 3. PDIR spectra from polycrystalline gold in aqueous 0.5 M Na_2SO_4 (points) fitted to Gaussian peak shapes (lines). Applied (sample) potentials are as shown in the figure; the reference potential was +0.8 V vs. Ag/AgCl.

Figure 4. PDIR data from polycrystalline gold in 0.5 M H_2SO_4 (points) fitted to Gaussian peaks (lines). Sample potentials are as shown and the reference voltage was +0.8 V vs. Ag/AgCl.

Figure 5. Plot showing experimental PDIR data (lines) and residuals from a Gaussian fitting routine (points) for (a) 0.5 M Na_2SO_4 and (b) 0.5 M H_2SO_4. The sample potentials in (a) and (b) were +0.3 V and +0.2 V, respectively; the reference voltage was +0.8 V vs. Ag/AgCl.

Figure 6. Plots of calculated PDIR spectral peak position (cm^{-1}) *vs.* applied potential for fitted data from 0.5 M Na_2SO_4 (triangles) and 0.5 M H_2SO_4 (circles). (a) Peak near 1100 cm^{-1}; (b) Peak near 1200 cm^{-1}.

Figure 7. Plots of calculated PDIR spectral intensity vs. potential for Gaussian fits of IR spectroelectrochemical data from (a) 0.5 M Na_2SO_4 and (b) 0.5 M H_2SO_4 on polycrystalline gold. In (a) a three-Gaussian fit was used, while in (b) a two-Gaussian model was employed. Filled squares: asymmetric sulfate peaks (~1200 cm^{-1}); filled circles: asymmetric bisulfate peaks (~1100 cm^{-1}); filled triangles: symmetric bisulfate peaks (~1050 cm^{-1}).

Figure 8. PDIR spectral results from a solution of 5 mM $CuSO_4$ in 0.5 M H_2SO_4 on polycrystalline gold. The reference potential was +0.8 V vs. Ag/AgCl, and the sample potentials are as shown in the figure.

Figure 9. Schematic showing proposed configurations of surface sulfate, bisulfate, and water on polycrystalline gold and electrodeposited copper surfaces as a function of applied potential. (a) 0.5 M Na_2SO_4. (b) 0.5 M H_2SO_4. (c) 5 mM $CuSO_4$ in H_2SO_4.

F1

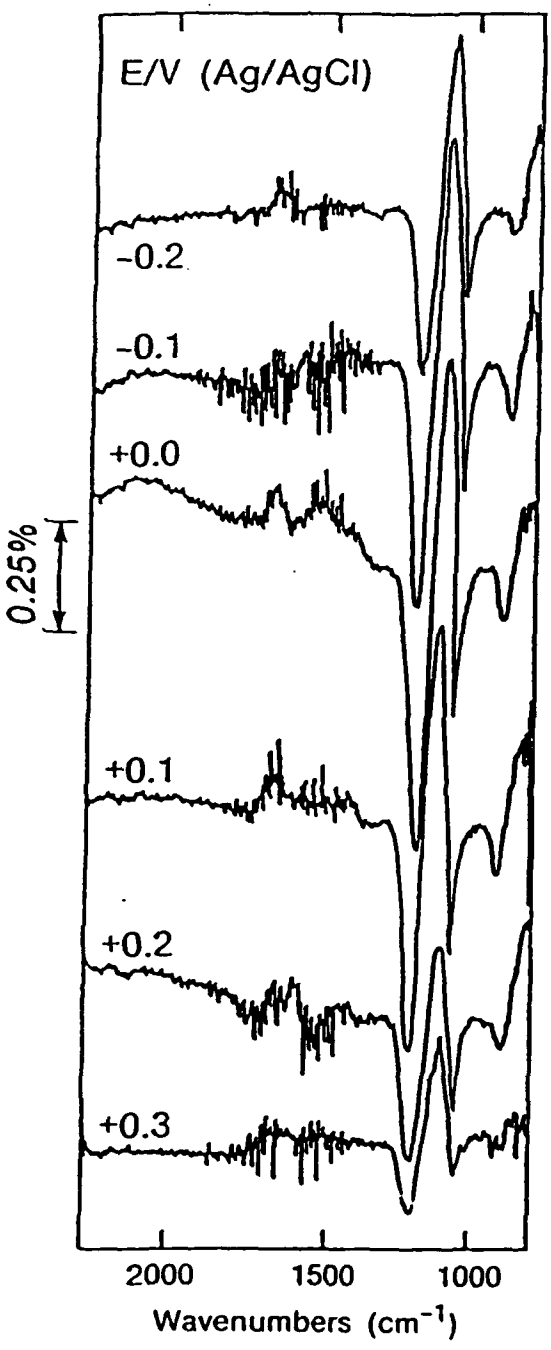

F2

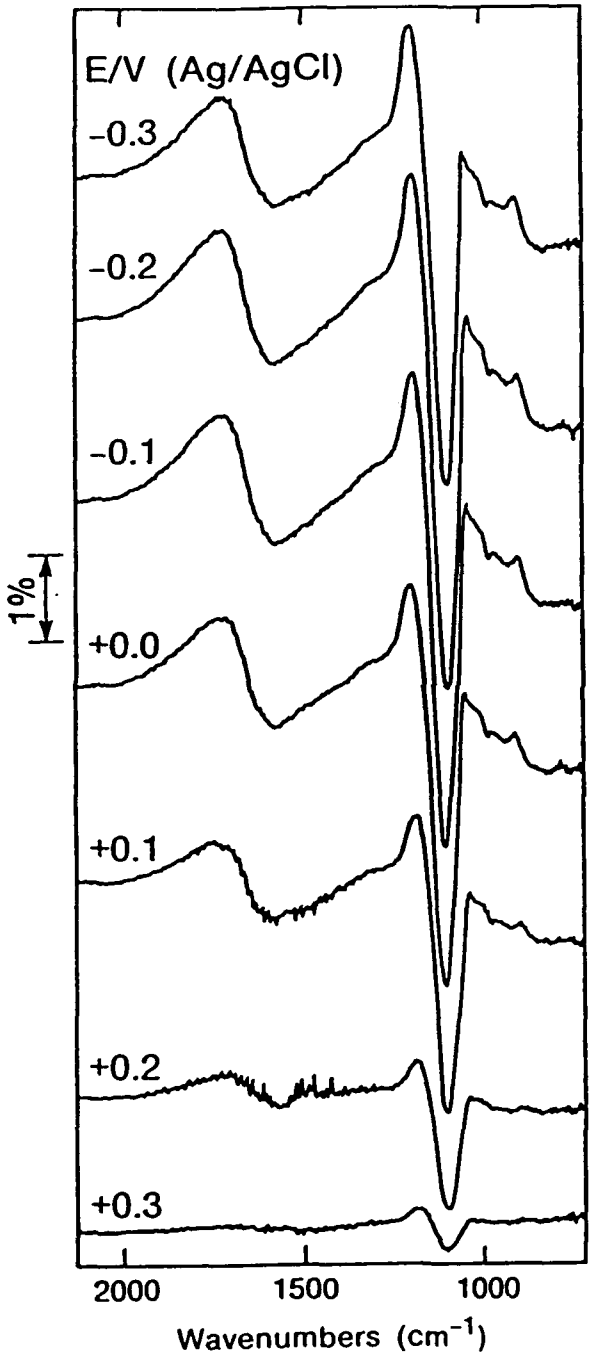

F3

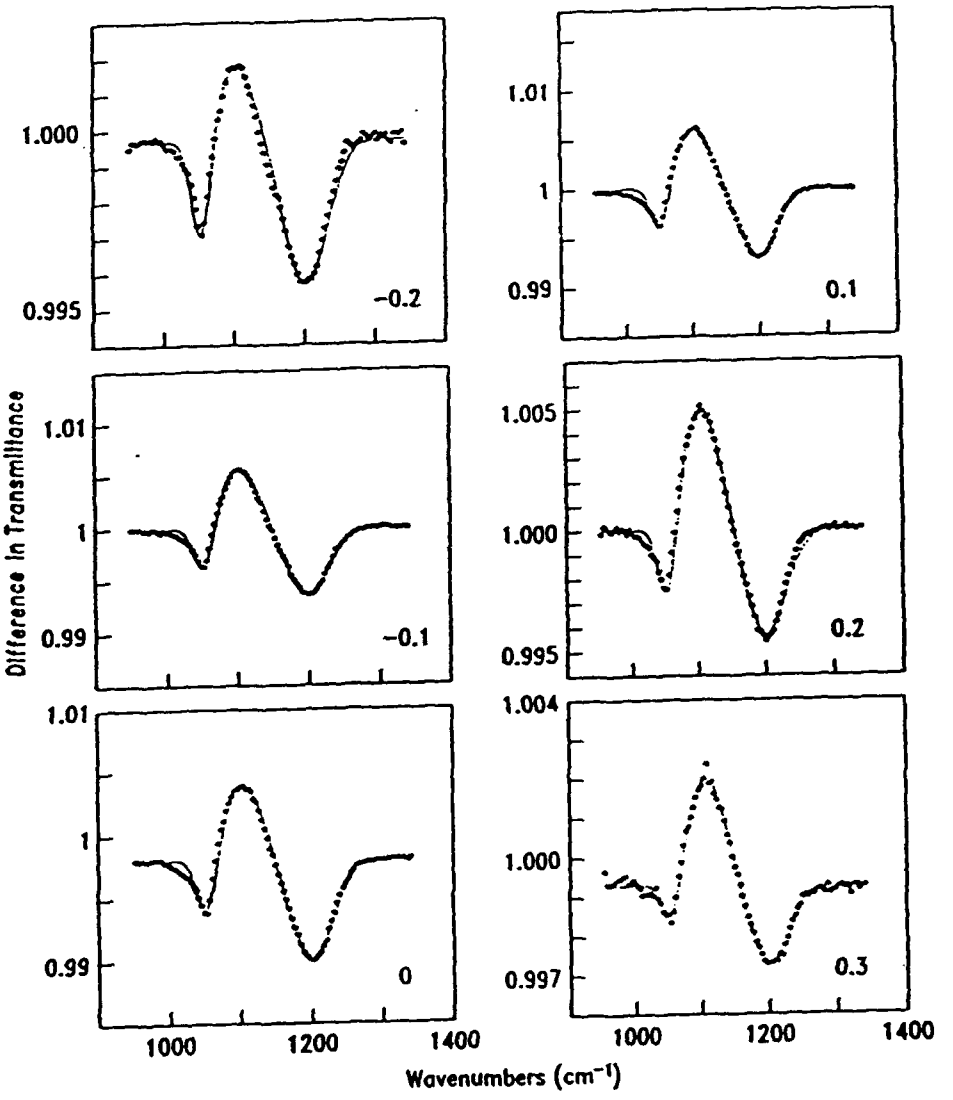
1.000
0.995
-0.2
1.01
1
0.99
0.1
1.01
1
0.99
-0.1
1.005
1.000
0.995
0.2
1.01
1
0.99
0
1.004
1.000
0.997
0.3
Difference in Transmittance
1000
1200
1400
1000
1200
1400
Wavenumbers (cm⁻¹)

F4

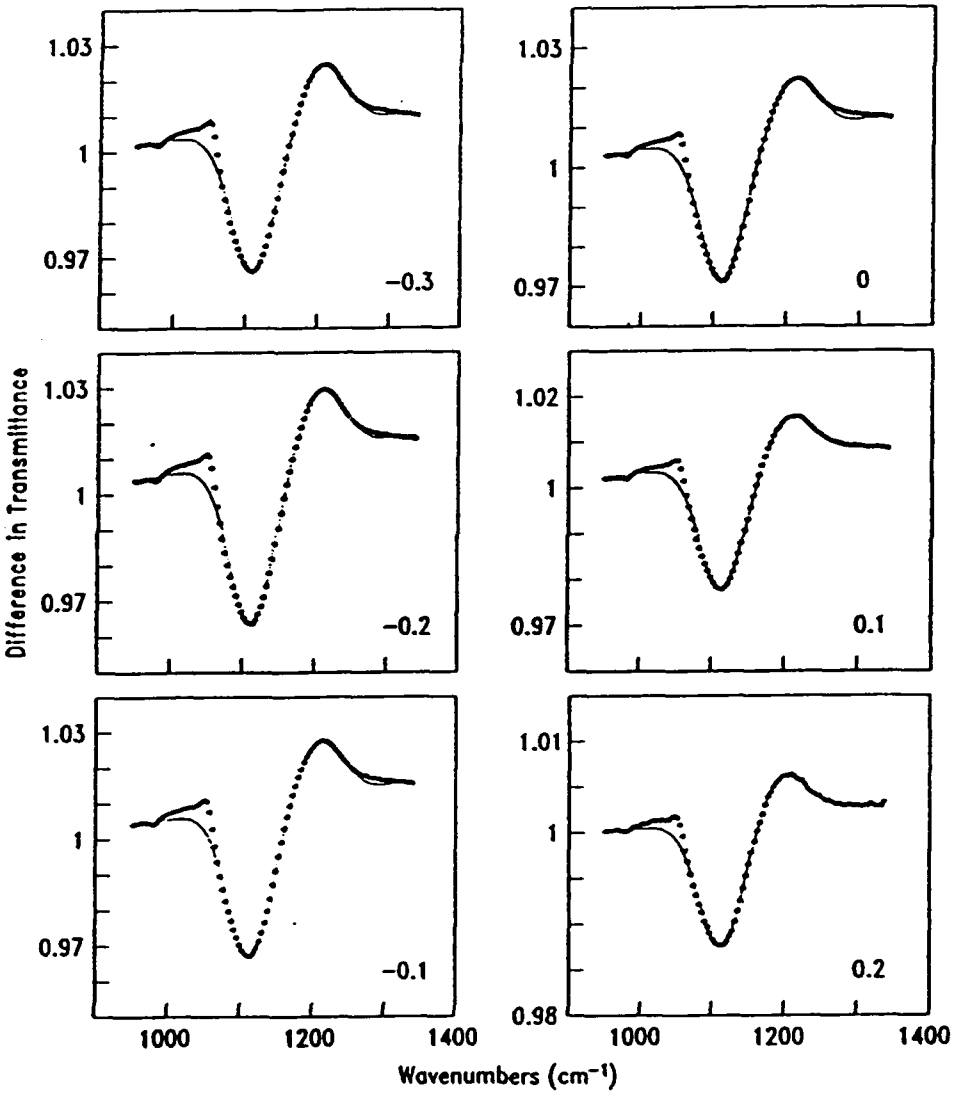
1.03
1
0.97
−0.3
1.03
1
0.97
0
1.03
1
0.97
−0.2
1.02
1
0.97
0.1
1.03
1
0.97
−0.1
1.01
1
0.98
0.2
Difference in Transmittance
1000
1200
1400
1000
1200
1400
Wavenumbers (cm⁻¹)

F5

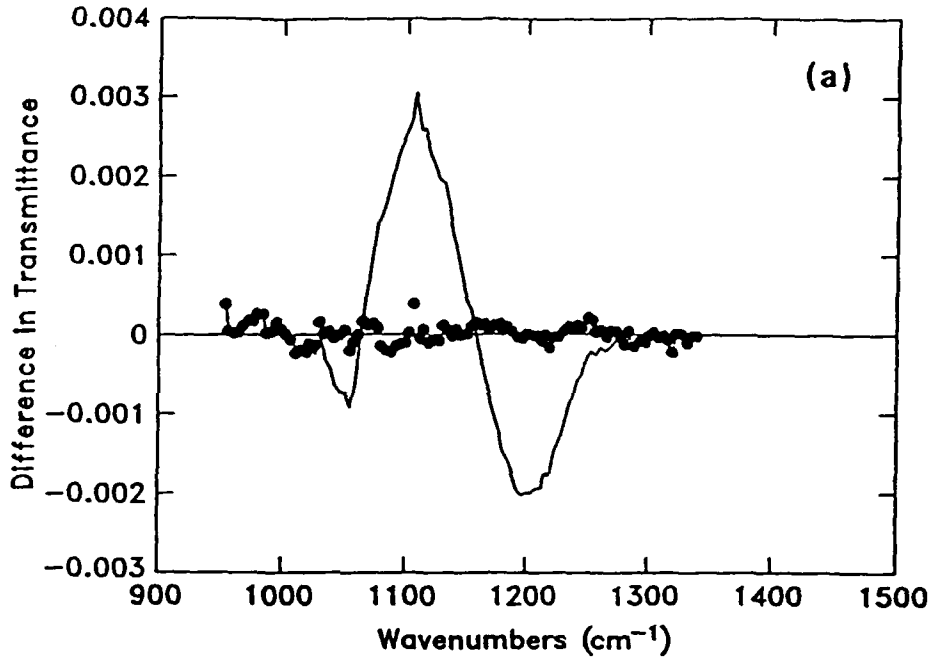
0.004
0.003
0.002
0.001
0
−0.001
−0.002
−0.003
Difference in Transmittance
(a)
900
1000
1100
1200
1300
1400
1500
Wavenumbers (cm⁻¹)

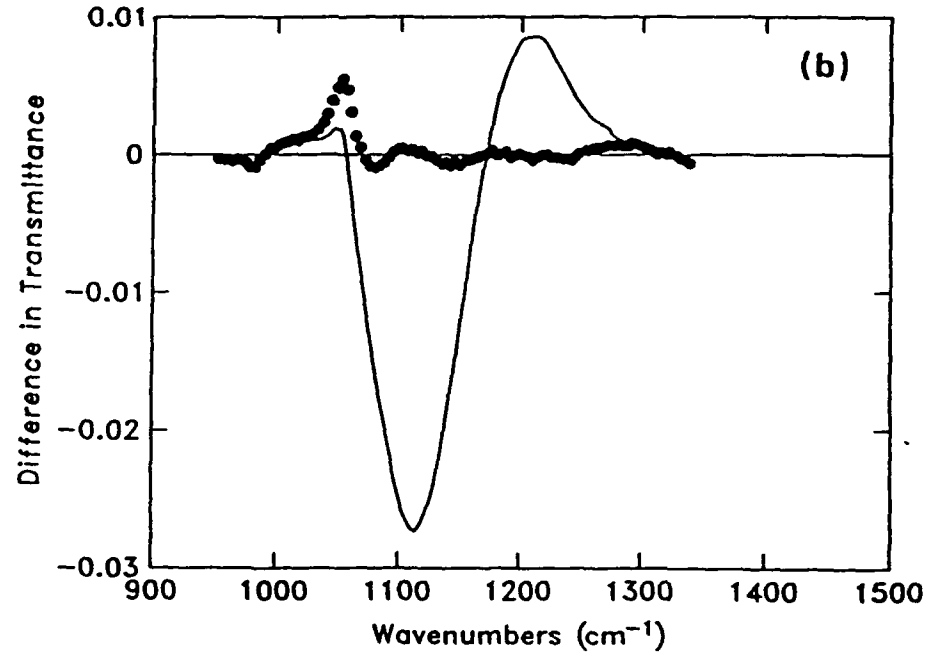
0.01
0
−0.01
−0.02
−0.03
Difference in Transmittance
(b)
900
1000
1100
1200
1300
1400
1500
Wavenumbers (cm⁻¹)

F6

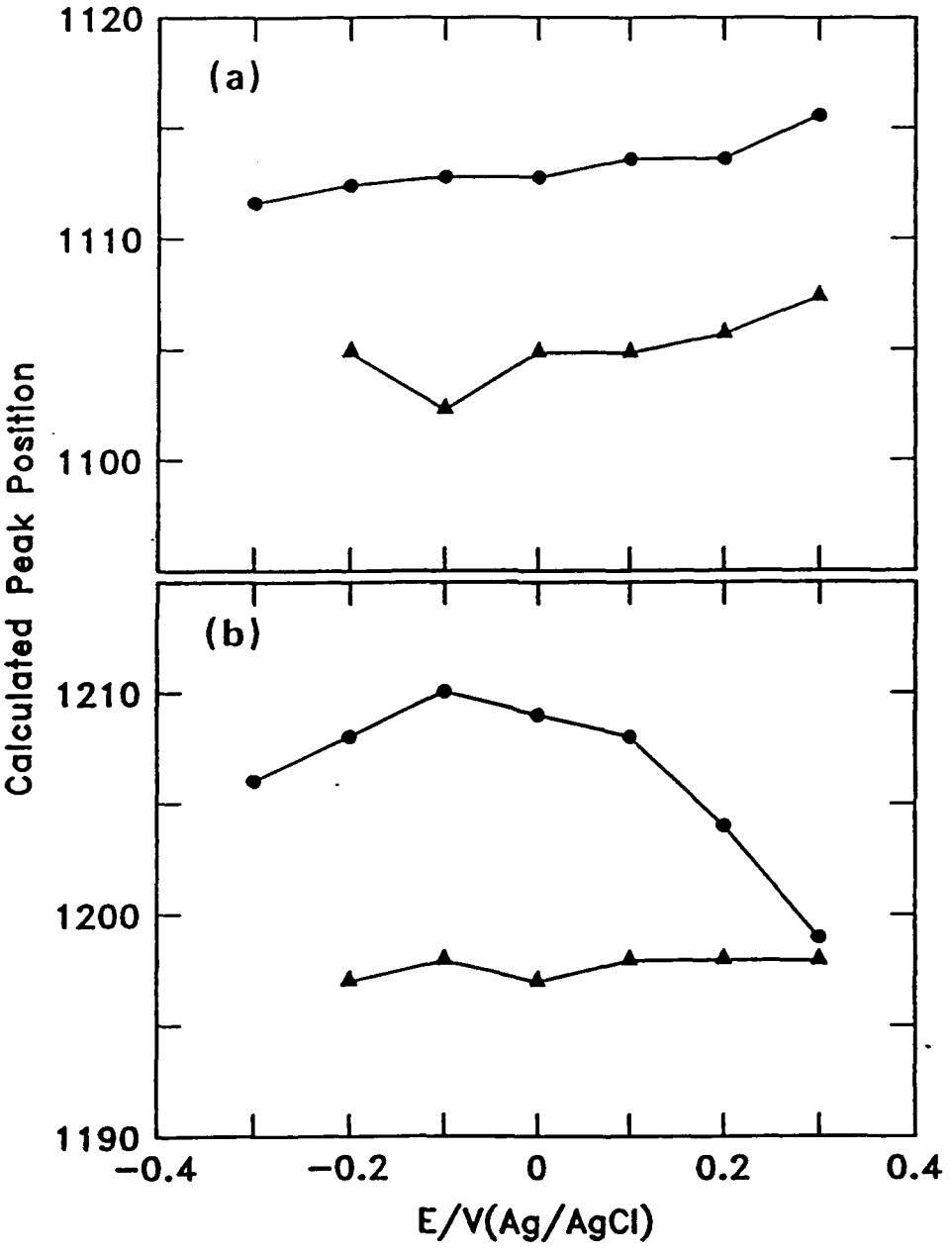
1120
1110
1100
(a)
(b)
1210
1200
1190
Calculated Peak Position
−0.4
−0.2
0
0.2
0.4
E/V(Ag/AgCl)

F7

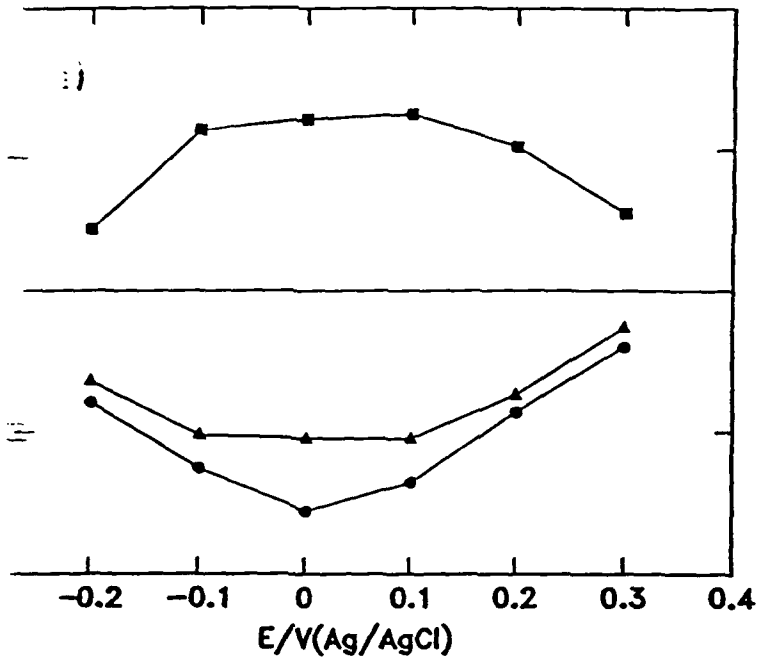

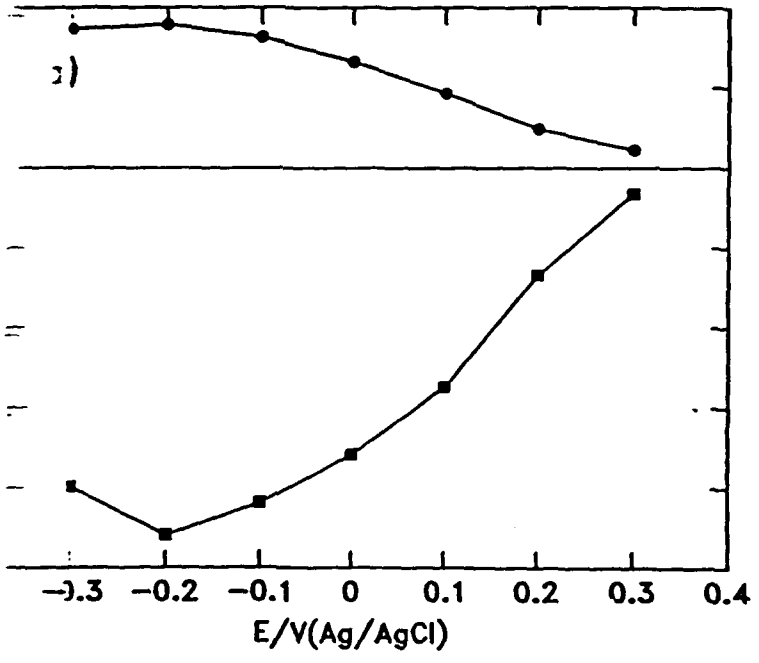

F8

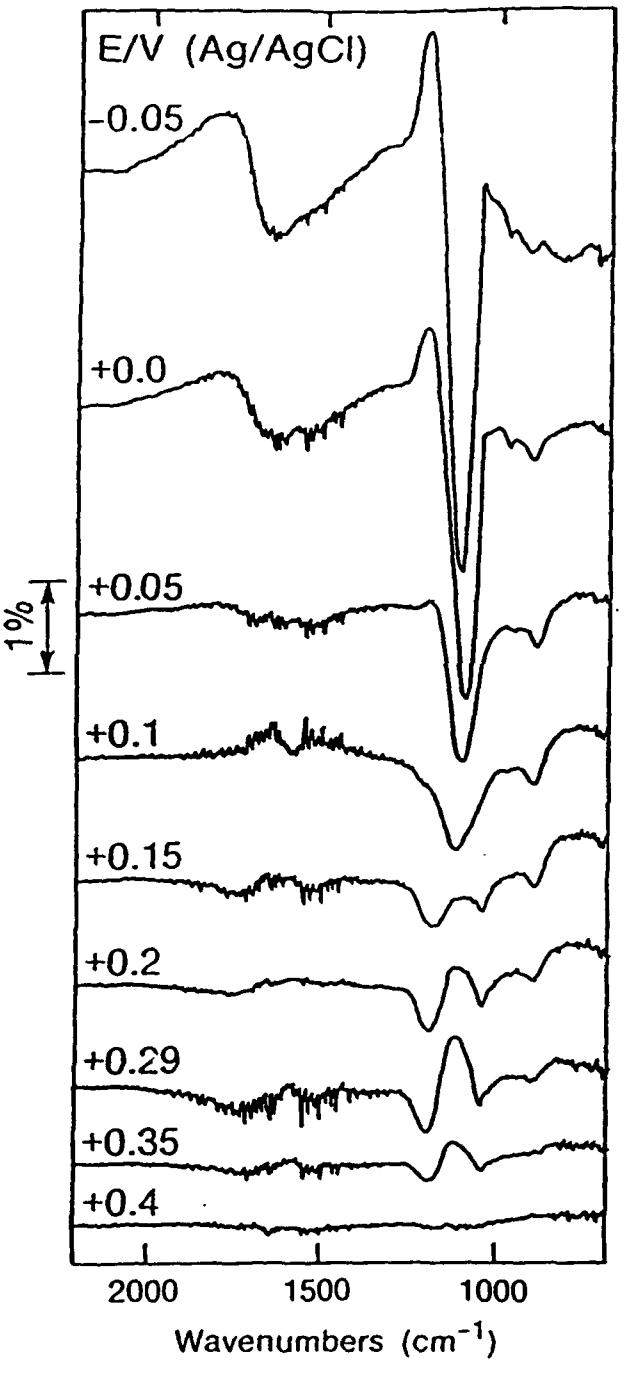
E/V (Ag/AgCl)
-0.05
+0.0
+0.05
+0.1
+0.15
+0.2
+0.29
+0.35
+0.4
1%
2000
1500
1000
Wavenumbers (cm^{-1})

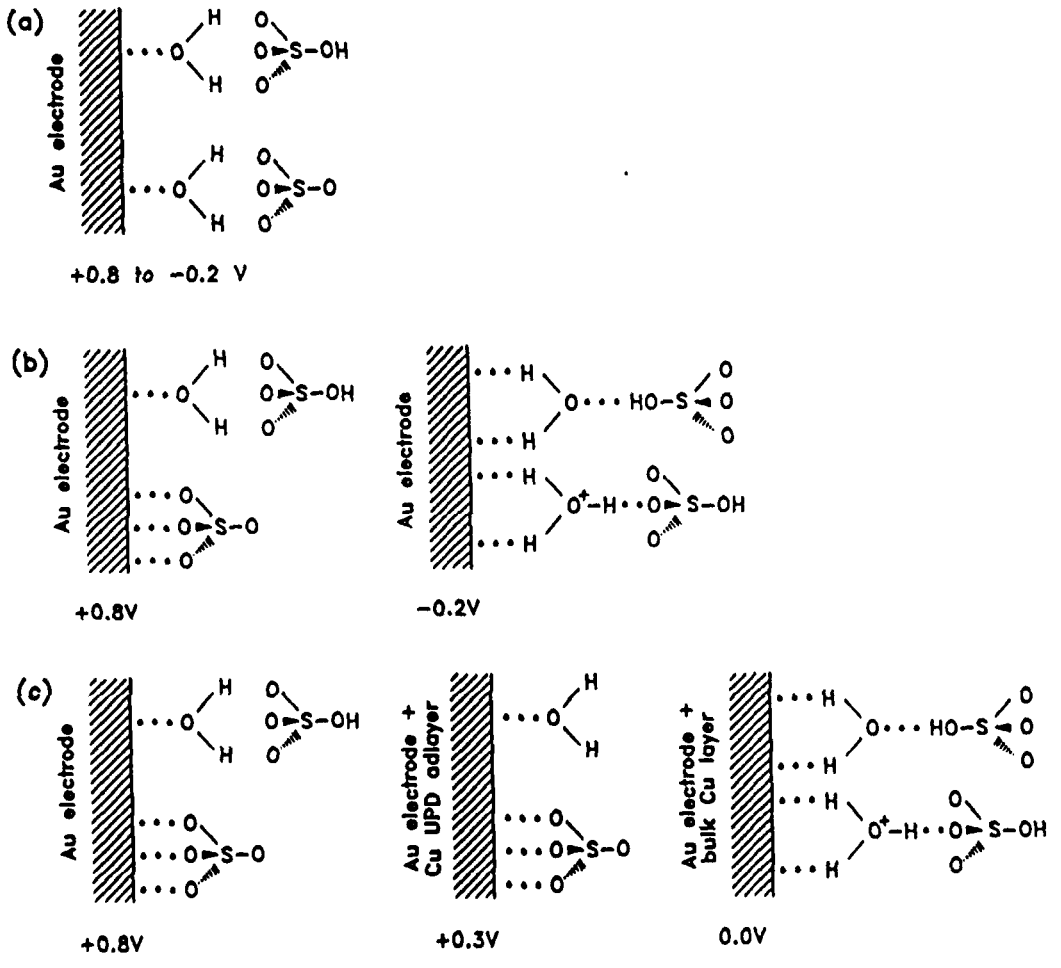
(a)
Au electrode
+0.8 to −0.2 V
(b)
Au electrode
+0.8V
Au electrode
−0.2V
(c)
Au electrode
+0.8V
Au electrode + Cu UPD adlayer
+0.3V
Au electrode + bulk Cu layer
0.0V

Fig